THE ASTROPHYSICAL JOURNAL, 398:62–68, 1992 October 10

THE X-RAY SPECTRUM OF ABELL 665

JOHN P. HUGHES
Harvard-Smithsonian Center for Astrophysics, 60 Garden Street, Cambridge, MA 02138
AND
YASUO TANAKA
Institute of Space and Astronautical Science, 1-1, Yoshinodai, 3-chome, Sagamihara-shi, Kanagawa 229, Japan
Received 1991 January 7; accepted 1992 April 14

ABSTRACT

The X-ray spectrum of the Abell 665 cluster of galaxies has been determined by the *Ginga* satellite. The spectrum can be well fitted by an isothermal model with $kT = 8.26(+0.95; -0.81)$ keV and metal abundance 0.49 ± 0.16. Joint analysis with lower energy spectral data from the *Einstein Observatory* is used to constrain the temperature distribution in the cluster. For a particular form of the polytropic temperature model we find the best fit to be the isothermal case, and we set an upper limit on the polytropic index of 1.35 (99% confidence). The virial mass of the cluster has been determined from both the X-ray data and the galaxy velocity dispersion. The mass estimates from the optical and X-ray analyses are fully consistent with each other. Abell 665 is found to be $0.82(+0.41; -0.26)$ times as massive as Coma if the two clusters are assumed to have the same spatial distribution of virial mass.

Subject headings: galaxies: clustering — intergalactic medium — X-rays: galaxies

1. INTRODUCTION

Abell 665 is a rich, distant ($z \sim 0.18$) cluster in the constellation Ursa Major. For some years now it has been the target of extensive radio observations and a strong decrement in the temperature of the cosmic background radiation, the signature of the Sunyaev-Zel'dovich (SZ) effect in the Rayleigh-Jeans portion of the background spectrum, has been observed from the cluster (Birkinshaw 1989). In this article we report primarily on an X-ray spectral study of A665. The intent of the investigation is to determine the average gas temperature of the cluster atmosphere, to set limits on the allowed temperature distributions, and to determine the cluster binding mass. We do this using data from the *Einstein Observatory* imaging proportional counter (IPC) and the large area counters (LAC) on the Japanese satellite *Ginga* (Makino et al. 1987). Birkinshaw, Hughes, & Arnaud (1991, hereafter BHA) employ these spectral results to determine the Hubble constant from an analysis of the SZ effect for this single cluster.

The decrement in the cosmic microwave background radiation due to the SZ effect is proportional to the line-of-sight pressure ($n_e T$) integral through the cluster. Thus any study of the SZ effect and use of it for distance determination requires an accurate representation of the gas density and temperature structure of the cluster atmosphere. The imaging instruments on board the *Einstein Observatory* have provided excellent information on the gas density distribution for a large number of galaxy clusters (e.g., Abrampoulos & Ku 1983; Jones & Forman 1984) and for A665 in particular. These data, however, were unable to define the temperature distribution or even to determine the mean gas temperature of most galaxy clusters.

Some previous studies of the SZ effect have attempted to compensate for the lack of temperature information by using measured galaxy velocity dispersions to estimate mean gas temperatures (e.g., Birkinshaw 1979; Boynton et al. 1982). This technique is rather unreliable given the large scatter on the observed correlation between temperature and velocity dispersion (Edge & Stewart 1991) and due to the possible presence of projection effects and/or subclustering which can strongly bias the velocity dispersion for any individual cluster. Other studies have employed both velocity dispersion data and X-ray spectra to infer the temperature distribution (White & Silk 1980) using the assumption of hydrostatic equilibrium and the underlying cluster virial mass distribution to connect the two observables.

Information on the binding mass of galaxy clusters is itself of astrophysical interest because of the presence of significant amounts of dark matter in these systems. We use our X-ray spectral data and the recently measured velocity dispersion from Oegerle et al. (1991) to estimate the cluster's virial mass. Our work finds that A665 is indeed massive, requiring large amounts of nonluminous matter to gravitationally bind the cluster. We compute the total cluster mass and compare it to the optical luminosity in the galaxies and the mass of X-ray–emitting hot gas. The values we obtain for these quantities for A665 are all very similar to the values found for the rich nearby Coma Cluster. The binding mass we derive is within a factor of 2 of the value used by Davidsen et al. (1991) to test the hypothesis that the dark matter associated with clusters of galaxies consists of decaying massive neutrinos as suggested by Sciama (1991, and references within).

We also consider polytropic models of the type introduced by Henriksen & Mushotzky (1986), i.e., where $T \propto n^{\gamma-1}$ while the density distribution is given by the isothermal-β form. This polytropic formulation is very convenient for the SZ study, since the functional form of the pressure integral remains the same as in the case of an isothermal distribution. We find that the X-ray data favor an isothermal distribution and that the maximum allowed polytropic index is 1.35.

As mentioned above, the IPC was able to produce images of cosmic sources in the 0.2–4 keV X-ray band. In BHA we present the results of a detailed analysis of the A665 image. The IPC was also able to obtain low-energy X-ray spectra at moderate resolution ($\Delta E/E \sim 1$ at 1 keV), which has been most useful for determining the absorbing column density to A665 and for constraining the amount of 1 keV temperature gas in

the cluster. The *Ginga* LAC is a mechanically collimated (approximately $1° \times 2°$ field of view) large area array (4000 cm^{-2}) of proportional counters with good sensitivity from 1.5 keV to 30 keV (Turner et al. 1989). It is the first instrument with the ability to determine the X-ray spectra of faint (10^{-11} ergs cm^{-2} s^{-1}) X-ray sources in this energy band. LAC data are quite good at determining the mean temperatures of clusters from the shape of the bremsstrahlung continuum emission and the mean elemental abundance from the strength of the Kα iron line near 6.7 keV. Joint analysis of the low-(IPC) and high-(LAC) energy X-ray spectra, such as we carry out here, allows us to constrain strongly the temperature distribution for the cluster and thereby allows us to set limits on the virial mass of the cluster.

In the next section we discuss the data reduction of the *Ginga* and IPC data. Isothermal and polytropic model fits follow in § 3. Section 4 discusses the virial mass estimates and § 5 concludes.

2. DATA REDUCTION

2.1. *Ginga LAC Data*

The A665 cluster of galaxies was observed by the LAC on the Japanese satellite *Ginga* on 1988 November 10. During the higher background period of the *Ginga* orbit, we carried out scanning observations. The source was clearly detected at the expected position of the cluster, and it was consistent with an unresolved source viewed by the *Ginga* collimator. No other sources were seen in the vicinity. The fitted peak counting rate in the LAC was 4.8 s^{-1} (1.7–9.3 keV).

Pointed observations of A665 were done during the lower background remote orbits. During this period over 20,000 s of data satisfied the following stringent data selection criteria and were included in the spectrum. The Earth elevation angle was required to be larger than 12°. Data from regions in the satellite orbit corresponding to higher background (such as the SAA passage and orbital regions with low cut-off rigidity) were rejected. We rejected data from segments in which the LAC high voltage was turned on or off. The angle from the LAC field of view and the Sun was greater than 90°, so contamination from solar X-rays was not a problem. After background subtraction the source yielded a counting rate in the LAC of 3.8 s^{-1} (1.7–9.3 keV). This is consistent with the scanning data since the pointing position of the LAC was offset from the cluster position by about 0°.3 to avoid a possible contaminating source [π(1) UMa]. The calculated collimator response at the X-ray position of the cluster was 0.785. There was no significant flux in the mid-layer of the LAC, and we consider only the spectrum from the top layer. In each pulse height (PH) channel a systematic error of 1% of the source signal was added in quadrature with the statistical error to account for uncertainties in the energy bin boundaries.

The gain of the LAC is monitored in flight using the Ag Kα line at 22.1 keV, which arises from fluorescence of cosmic X-ray background photons and cosmic-ray particles in the silver coating on the LAC collimator. For this observation, we fitted the Ag Kα line energy for each of the eight individual detectors in the top layer and from these computed an average response function which was used subsequently in the model fitting. Note that the overall average gain was such that the Ag Kα line fell in PH channel 35.07, which lies within the nominal range of gain values (between 35.0 and 35.2; S. Takano, private communication). The 1 σ uncertainty in the statistical determination of the line centroid was ± 0.06 keV. We use this value below to represent the systematic uncertainty in the LAC gain. The linearity of the LAC energy scale was determined prelaunch, and it was assumed that this remained stable during the mission.

The background of the LAC has been studied in great detail (Hayashida et al. 1989) and for sources at the flux level of A665, proper background subtraction is the single most important consideration. For background subtraction during the A665 observation, we employed two techniques: (1) a direct method, which uses background data from a blank-field pointing on an adjacent day and (2) the background model developed by Hayashida et al. We found that the two techniques yielded slightly different results for best-fit values, although the error intervals on those parameters overlapped. Given that the derived spectra were reasonable and that there was no reason to prefer one method over the other (each has its advantages as well as disadvantages), we determined to average the spectra obtained by the separate techniques. We note that the differences between the fitted results in the two cases are at the level of the background-subtraction uncertainty (which we explicitly examine below).

Hayashida et al. determined that the 1 σ uncertainty in their background subtraction technique corresponded to a 2–10 keV count rate of 0.86 s^{-1}, which they claim arises partly from spatial fluctuations in the diffuse X-ray background (about two-thirds of the total) and partly from other systematic effects in estimating the induced-particle background (the remaining one-third). We have used our scanning data to establish an uncertainty in background subtraction appropriate to this observation of A665. The data from regions of the scan which did not include the cluster were analyzed using the same background-subtraction model as used for generating the source spectrum. We found that there was a residual net positive counting rate of about 0.4 s^{-1} from this region. This is the value which we use below to represent the systematic uncertainty in the background subtraction since it corresponds more closely to the local spatial vicinity of the cluster and is more nearly contemporaneous with the actual source observation.

We have summed the data from the top layer for the eight individual detectors to form the *Ginga* spectrum, which we show in Figure 1. We consider only the spectrum up to about 13 keV; above this energy the signal is dominated by residual systematic errors in background subtraction at a level of about 0.01 counts s^{-1} keV^{-1}. All quoted results are based on the summed spectrum in Figure 1.

2.2. *Einstein IPC Data*

The *Einstein* imaging proportional counter (IPC) observed A665 for 6430.8 s (dead-time corrected exposure time) on 1979 October 9. An extended source with a background-subtracted counting rate of 0.293 ± 0.007 s^{-1} (over the energy band 0.23–4.1 keV and within a radius of 8′) was clearly detected at a position of $8^h26^m25^s$, 66°1′21″ (1950). This is about 3′ south of the Abell (1958) position. In this paper we concentrate on the spectral analysis of the IPC data; further details of the imaging data and a complete spatial analysis are given in the accompanying article (BHA). However, we wish to highlight the following points: the cluster X-ray surface brightness distribution is well described by the isothermal-β model with $R_{core} = 1'.6$ and $\beta = 0.66$. Furthermore, the cluster can be considered to follow this profile out to radii of 6′.0, 5′.0, and 4′.2 at confidence levels of 68%, 90%, and 99%, respectively. The *Einstein* high-

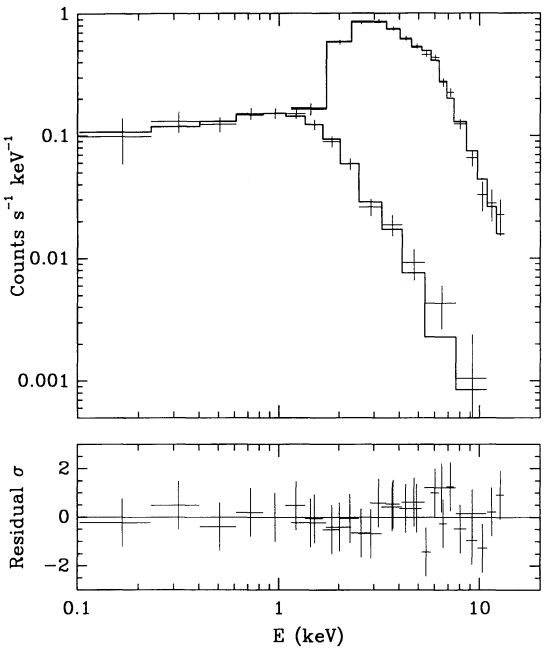

FIG. 1.—The X-ray spectrum of A665 as observed by the *Einstein Observatory* IPC and the *Ginga* LAC. The best-fitting isothermal model is also shown.

resolution image of the cluster is entirely consistent with this model and in particular, shows no emission from a pointlike source near the core of the cluster. The lack of evidence for a central surface brightness spike strongly limits the presence of any cooling flow component in this cluster. Detailed analysis of this data set is limited by the low signal-to-noise ratio (S/N) of the observation; the cluster was detected at only the 7 σ confidence level. See BHA for more details on the X-ray imaging analysis.

Three unresolved sources beyond about 15′ from the cluster center were detected by the IPC at the following positions: $8^h24^m12^s$, 66°12′6″; $8^h28^m42^s$, 66°14′4″; and $8^h28^m43^s$, 66°1′21″ (1950 positions) (Harris et al. 1990). The first source had a very soft IPC spectrum (hardness ratio of $-0.43[+0.14; -0.13]$, corresponding to a temperature of about 0.2–0.3 keV, which does not contribute to the *Ginga* spectral band. The latter two sources were identified with active galactic nuclei (AGN) (Gioia et al. 1990) and had 0.3–3.5 keV X-ray fluxes of 2.48×10^{-13} ergs cm^{-2} s^{-1} and 4.90×10^{-13} ergs cm^{-2} s^{-1}, respectively. Because of the large field of view of the *Ginga* collimator (1° by 2° FWHM), it was not possible to avoid these sources in the *Ginga* observation. However, in the *Einstein* IPC band the combined flux of these sources was nearly an order of magnitude smaller than the flux from the cluster. On the other hand, the X-ray spectrum of the average AGN is different enough from that of the average cluster of galaxies that some effect of these confusion sources might be evident, especially in the high energy X-ray band of *Ginga*. We investigate the effect of these sources on the interpretation of the *Ginga* spectrum in our analysis below.

Since the cluster is significantly extended, background subtraction of the A665 IPC spectrum required use of a separate gain-matched source-free field. For this purpose we used a deep survey field (I31) with a gain of 18.77 versus 17.43 for the A665 pointing. The background spectrum was scaled to the source spectrum by the ratio of live times. This scaling value was sufficient to approximately zero out the background in the source field near the edge of the detector, far from any possible emission from the cluster. We also employed a different deep survey background field (I3670, gain: 16.48); all derived results were consistent at the 68% confidence level with those using field I31 for background. The background rate in the IPC was known to vary from field to field by of order 20%. To incorporate this uncertainty, we included an additional 20% of the background rate in quadrature with the statistical error in each pulse height (PH) channel. An additional systematic error of 3% of the source rate in each PH channel was added in quadrature to the combined statistical and background systematic error. Due to the significant background systematic error, the maximum S/N was obtained when the spectrum was extracted from within a radius of 8′ from the cluster center. The IPC X-ray spectrum of A665 is shown in Figure 1.

3. ISOTHERMAL AND POLYTROPIC MODEL FITS

Our aim here is to convert the observed X-ray spectra shown in Figure 1 into information about the temperature structure of the cluster. The density structure can most accurately be determined through analysis of the X-ray images of A665; as we mentioned above, this is done in BHA. In § 3.1 immediately following we focus on constraining the spectral parameters, i.e., the hydrogen column density to the source, the average iron abundance, the average gas temperature, and the emission measure, under the assumption that the cluster is isothermal. We give best fit values and error ranges for each parameter. Each parameter is essential, since the conversion from IPC counts to equivalent hydrogen number density used in BHA depends implicitly on the column density, temperature, and iron abundance. Even the relative normalization between the IPC and *Ginga* data sets is useful, since it allows us to assess the systematic uncertainty in the overall flux calibration of the two instruments. The temperature value itself is particularly important since it enters linearly into the SZ effect. In § 3.2 we consider polytropic temperature distributions of the form introduced by Henriksen & Mushotzky (1986), i.e., where $T \propto n^{\gamma-1}$, while the density distribution is given by the isothermal-β form. This polytropic formulation is very convenient for the SZ study, since the functional form of the pressure integral remains the same as in the case of an isothermal distribution. In addition at this point we show how important the combination of IPC and *Ginga* data sets is for constraining nonisothermal temperature distributions in distant clusters.

3.1. *Isothermal Temperature Distributions*

The IPC and *Ginga* data sets were simultaneously fitted to redshifted optically thin collisional ionization equilibrium thermal bremsstrahlung models (Raymond & Smith 1977; J. C. Raymond, private communication; hereafter RS). We introduce a relative normalization parameter to account for numerous possible differences between the IPC and *Ginga* in the area of overall flux determination. Some effects which might influence this quantity include the absolute flux calibration of both instruments, background subtraction, the *Ginga* collimator transmission function, the spatial integration region for the IPC data, and the hydrogen column density to the source. Both this parameter and the hydrogen column density were allowed to be variable. For the metal abundance, the elements C, N, O, Ne, Mg, Si, S, Ar, Ca, Fe, and Ni were varied in unison, while the [He]/[H] ratio was fixed at 0.085. The best-fit values for the parameters of this model are shown in Table 1

TABLE 1

BEST-FIT PARAMETERS: RS MODEL

Parameter	Best-fit Value[a]
Emission integral ($n_H^2 V$)[b] (10^{68} cm^{-3})	1.12 ± 0.05
kT (keV)[c]	$8.26(+0.95; -0.81)$
Abundance[d]	0.49 ± 0.16
n_H (10^{20} atoms cm^{-2})	$4.1(+2.8; -1.7)$
Relative norm (IPC/*Ginga*)	0.95 ± 0.08
χ^2 (dof)	13.4(25)

[a] Statistical errors at 90% confidence.
[b] Assumes $z = 0.18144$, $H_0 = 50$ km s^{-1} Mpc^{-1}, and $q_0 = 0.5$.
[c] Source temperature.
[d] Relative to cosmic: [Fe]/[He] $= 4 \times 10^{-5}$.

and the best-fit spectrum is plotted in Figure 1. These results are for a fixed redshift value of 0.18144 (Oegerle et al. 1991). We also determined the redshift from our data by fitting (of course, it is the strong iron line which gives us our sensitivity to this parameter) to be 0.154 ± 0.039 (90% confidence), consistent with the optical value. The fitted hydrogen column density is consistent with the Stark et al. (1984) value of 4.3×10^{20} atoms cm^{-2}.

The best-fit relative normalization between the data sets (IPC/*Ginga*) is some 5% smaller than the value expected based on calculating the *Ginga* collimator transmission alone. This is largely due to the region of integration for the IPC spectrum. When we integrate the best fit isothermal-β model for the IPC surface brightness profile within a radius of 8′ and compare it to the same calculation within 16′, we find that there should be about 12% less flux from the smaller region. For this calculation to be relevant, of course, one must assume that the cluster follows the modeled surface brightness law out to 16′, about 10 core radii. If anything, the surface brightness should fall off more rapidly at large radii, since the exact King (1966) model does differ from the isothermal-β model approximation in just this fashion. However, recent results from the *ROSAT* all-sky survey show that the Coma Cluster follows the isothermal-β surface brightness model out to a radius of about 10 core radii (Briel, Henry, & Böhringer 1991). We consider the 12% value to be a lower limit to the decrease in flux we might expect to see in the IPC spectrum compared to the *Ginga* one. In light of these points, we consider the agreement between the IPC and *Ginga* data sets to be excellent and we suggest that it validates our background subtraction and the absolute flux calibration of the two instruments. Furthermore, it establishes a systematic uncertainty of about 5% in the overall flux calibration of each instrument.

The 2–10 keV flux of A665 (corrected for pointing position) is 1.0×10^{-11} ergs cm^{-2} s^{-1} which implies a luminosity of 1.5×10^{45} ergs s^{-1} (for $H_0 = 50$ km s^{-1} Mpc^{-1}, $q_0 = 0.5$). Correlations of X-ray luminosity and gas temperature for samples of galaxy clusters have been given by a number of authors now (Mushotzky 1988; Edge 1989; Hatsukade 1989). Our measured gas temperature and X-ray luminosity for A665 are consistent with the correlations given by these authors. We estimate the cluster velocity dispersion to be 1050 km s^{-1}, based on the measured X-ray temperature and employing the correlations in Edge (1989). This is in excellent agreement with the Oegerle et al. (1991) measurement of $1201(+183; -126)$ km s^{-1}.

Before investigating nonisothermal temperature distributions, we would like to examine the dependence of some of our present results on the uncertainty in gain and background subtraction for the *Ginga* data. We generated results for plus and minus 1 σ variation in gain and background subtraction, using the values determined in § 2. The best-fit temperature changed by ± 0.15 keV when the gain was varied and by $(+1.32; -1.19)$ keV when the background was varied (first value comes from subtracting less background, second value from more background). The iron abundance was much less sensitive to these variations, changing by only ± 0.006 (gain) and $(-0.007; +0.019)$ (background). The relative normalization changed by $(-0.069; +0.082)$, and the flux by $\pm 1.4 \times 10^{-12}$ ergs cm^{-2} s^{-1} when background was varied. It is clear that some of these systematic errors are comparable in importance to the statistical errors on the measured parameters. Varying the background for the IPC data was significantly less important than for the *Ginga* data since the background in this case represents a considerably smaller fraction of the overall count rate.

We have investigated the contribution to the *Ginga* spectrum of the two AGN observed in the IPC image. When a power-law model with photon index -1.7 is included with the RS thermal model, the best fit for the normalization of the power-law component turns out to be zero. If the flux of this power-law component is fixed at the value inferred from the IPC observation (summing the contributions of the two sources), then the best-fit temperature of A665 decreases by 0.39 keV and the elemental abundance increases by 0.047. These errors are dominated by the other systematic and statistical errors discussed above and shown in Table 1.

3.2. *Polytropic Temperature Distributions*

In this section of the paper we relax the assumption that the cluster temperature distribution is isothermal. We assume that the distribution is polytropic and that the underlying density distribution is given by the isothermal-β model with $R_{\rm core} = 1.'6$ and $\beta = 0.66$. We have fixed the hydrogen column density and the relative normalization to the best-fit values from the isothermal model. Note that our results concerning the degree of nonisothermality in A665 do not change significantly if we fix the column density to the Stark et al. (1984) value and the relative normalization to the calculated *Ginga* collimator transmission value.

Figure 2 shows results from fitting the combined IPC and *Ginga* data sets to the polytropic model. Contours of constant χ^2 for central temperature versus polytropic index (γ) are shown at the 68%, 90%, and 99% confidence level. The best fit is an isothermal model and we can exclude an adiabatic temperature distribution at very high confidence. A meaningful constraint on the polytropic index is not possible when either the IPC or *Ginga* data set is analyzed separately. It is possible only because of the broad energy coverage of the combined data sets.

4. VIRIAL MASS MODELS

Here we use the X-ray spectral data and the velocity dispersion of the galaxies to determine a likely value for the virial mass of A665. We follow closely the technique developed by Hughes (1989) (see also The & White 1986 and Merritt 1986) in a detailed study of the mass distribution of the Coma Cluster. This technique assumes a parameterized functional form for the virial mass distribution from which the gas temperature

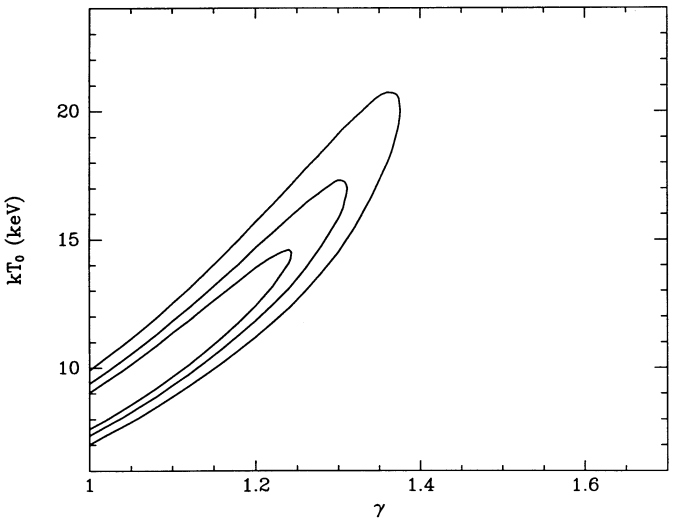

FIG. 2.—Contours of constant χ^2 for the polytropic model at the 68%, 90%, and 99% confidence level. The central temperature is plotted vs. the polytropic index γ.

distribution and the velocity dispersion can be calculated (see below). For the Coma Cluster, it was possible to explore the effect of using different functional forms for the spatial distribution of the binding mass; however, the optical and X-ray data for A665 are considerably less extensive than that from Coma and thus we have decided to fix the shape of the A665 mass distribution and only determine its overall normalization. For ease of comparison between Coma and A665, we have chosen the mass-follows-light model for Coma, which is the preferred binding mass distribution from Hughes (1989). Specifically we assume $\rho_b = \rho_0[1 + (r/298\ \mathrm{kpc})^2]^{-1.36}$ (The & White 1986) and determine limits on the central concentration of the binding mass distribution, ρ_0. Note that this distribution is somewhat different from both the A665 gas distribution (core radius 380 kpc) and the galaxy distribution (core radius 530 kpc; Dressler 1978), although the latter quantity is not known as precisely.

Even for a well-studied cluster like Coma, Hughes (1989) showed that uncertainties of $\pm 50\%$ in the total mass are possible when this method is applied. This is in addition to uncertainties arising from the model assumptions: e.g., that the gas is in hydrostatic equilibrium, the system is spherically symmetric, there is no substructure in the galaxy distribution, and the galaxy velocity distribution is isotropic. There is evidence for substructure in both the galaxy (Geller & Beers 1982) and gas (BHA) distributions of A665, which suggests that our results on the cluster binding mass could be subject to considerable uncertainty. However, the mass values we derive from the galaxy dynamics and the gas temperature are fully consistent with each other at the 68% confidence level, perhaps indicating that the observed substructure does not play too strong a role in biasing the mass measurement for this cluster.

4.1. *X-Ray Derived Virial Mass*

The X-ray analysis begins with the equation of hydrostatic equilibrium $\nabla P = -\rho_g \nabla\Phi$, which can be expressed as a first-order differential equation in gas temperature T

$$\frac{dT}{dR} = -\frac{1}{\rho_g}\frac{d\rho_g}{dR}T - \frac{4\pi\mu m_{\mathrm{H}} G}{k}\frac{M(R)}{R^2}. \quad (1)$$

$M(R)$, of course, is the total virial mass contained within radius R, obtained by integrating ρ_b and ρ_g is the gas density distribution; we use the isothermal-β model with parameter values determined from the *Einstein* X-ray imaging observations and given above (§ 2.2). We do not impose an explicit boundary condition on the temperature distribution (e.g., requiring the temperature to approach zero at infinity), but instead allow the X-ray spectral data to constrain it. We have chosen to represent this boundary condition on temperature as the emission-measure-weighted average temperature, kT_{AVE}. This gives us a two-parameter family of solutions for the temperature distribution: ρ_0 and kT_{AVE}, which are to be constrained by the X-ray spectral data.

We constructed a large grid of spectral models with varying ρ_0 and kT_{AVE}. For each set of parameters, a model temperature distribution was first calculated by solving equation (1). Next the model X-ray spectrum was built up by summing the spectra from single temperature RS thermal models, weighted by the appropriate relative emission measure at each temperature. Four more parameters were required to obtain acceptable fits to the joint IPC/*Ginga* spectral data: the overall emission measure, the metal abundance, the interstellar column density, and the relative normalization between the IPC and *Ginga* spectra. As was done for the polytropic temperature models mentioned above, we fixed the hydrogen interstellar column density and the relative normalization to the best-fit values from the isothermal fit. For this model there are as many free parameters (six) as for the polytropic temperature model, which itself includes only one more free parameter than the isothermal model.

The results are shown in Figure 3 as χ^2 contours at 68%, 90%, and 99% confidence for two interesting parameters. The

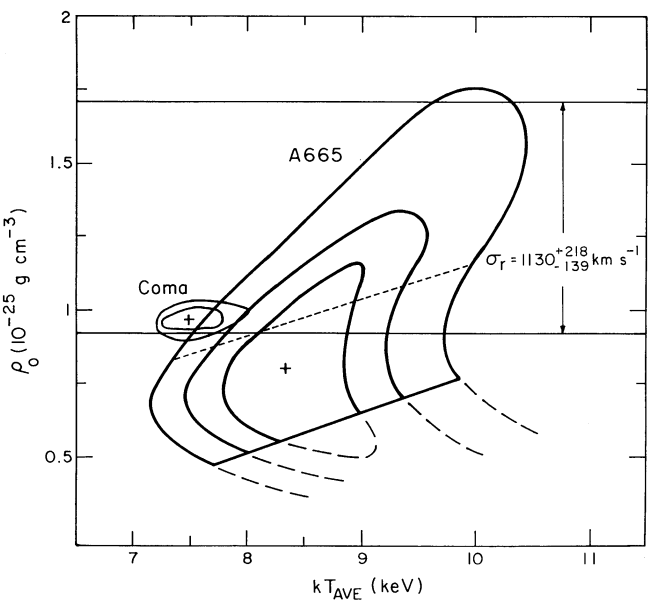

FIG. 3.—The virial mass of A665. The central concentration of the binding mass distribution (ρ_0) is plotted vs. the mean gas temperature of the cluster. The closed contours represent the region allowed by the X-ray data at 68%, 90%, and 99% confidence. The sloping dashed line within these contours separate the two classes of temperature solutions (see text). The binding mass of A665 derived from the galaxy velocity dispersion is shown as the band stretching along the temperature axis. For reference, the region of parameter space for the binding mass of the Coma Cluster is shown as the small contours to the left (90% and 99%).

central concentration of the binding mass distribution ρ_0 is plotted as the ordinate and the emission-measure-weighted average temperature is plotted as the abscissa. For A665, the constraints from the X-ray spectra have been augmented by the additional consideration that the external pressure not exceed a given value, which we have taken to be 0.001 cm^{-3} keV at the outer boundary of our model (about 10 Mpc). This constraint limits models with large positive radial temperature gradients, occurring for small values of central concentration. These are strictly speaking pressure-bounded models, in which the temperature rises to match the falloff of gas density and the pressure reaches a constant nonzero finite value at large radii. We have chosen a very conservative limit in this case corresponding to an external pressure no less than about 2% of the central value. Since this value is somewhat "soft," we have extended our contours (as dashed lines) beyond the limit. In the figure we also mark the line corresponding to the boundary between gravitationally bounded models and pressure-bounded models (the small-dashed straight line extending through the contours). Below the line the temperature rises to large values at large radii. These models could potentially correspond to situations where there is still infall in the cluster at large radii. Above this line the temperature drops to zero at large, but finite, radii, effectively defining the boundary of the cluster gas distribution. This boundary occurs at progressively smaller radii as ρ_0 increases. The fact that we see emission in the X-ray image out to a certain radius potentially allows for an additional constraint on the models. In the current situation this turns out not to be effective, since the boundary lies beyond 4.'2 for all accepted models.

The numerical value of the binding mass as derived from the X-ray spectrum is $\rho_0 = 0.80(+0.13; -0.18) \times 10^{-25}$ g cm^{-3} where the error is at the 68% confidence level for a single interesting parameter.

The two small contours near the left-hand side of the figure show the results for the binding mass of Coma at 90% and 99% confidence (Hughes 1989). The average temperature of A665 is about 1 keV higher than that of Coma. Although the best-fit value for the mass of A665 is 0.82 times that of Coma, the 90% confidence range on mass allows for A665 to be from 0.56 to as much as 1.23 times the mass of Coma. Yet if we require that the temperature distributions be approximately the same for the two clusters, then the virial mass of A665 is very nearly the same as Coma.

4.2. *Optically Derived Virial Mass*

The determination of the cluster virial mass from galaxy dynamics rests on the Jeans equation which we write as

$$\frac{d\rho_G \sigma^2}{dR} = -\frac{G\rho_G M(R)}{R^2} . \quad (2)$$

The galaxy distribution is ρ_G and the velocity dispersion, σ, is assumed to be equal in the radial and tangential directions, i.e., isotropic orbits. We set σ to zero at the boundary of the cluster, chosen to lie at a large radius ($\sim$50 Mpc). We have assessed the effect of reducing this boundary radius to 10 Mpc and find that our derived masses increase slightly (about 7%) in this situation. The galaxy spatial distribution is taken from Dressler (1978): $\rho_G \sim [1 + (R/530 \text{ kpc})^2]^{-1}$. Integration of equation (2) for each value of ρ_0 yields the radial run of σ, which is projected to the line of sight and averaged over an appropriate region of the cluster to yield the total cluster velocity dispersion. As we have formulated the problem, there is only one unknown parameter, ρ_0, to be determined by the measured velocity dispersion.

Current data on the galaxy dynamics of A665 consist of radial velocities for 33 cluster member galaxies from Oegerle et al. (1991), which were used to determine the total projected velocity dispersion: 1201(+183; −126) km s^{-1}. We compared the radial distribution of these galaxies with that expected from Dressler's profile and found a pronounced deficit of galaxies in the Oegerle et al. sample beyond about 7.'5. Thus the total data set (out to a radius of $\sim$20′) is demonstrably not a representative sample of the galaxy distribution of A665. However, the 23 galaxies within 7.'5 of the X-ray–determined cluster center did accurately follow the expected profile and the velocity dispersion for this limited sample was not significantly different: 1130(+218, −139) km s^{-1}. Although we feel that this subset is more representative of the cluster as a whole, our main reason for selecting it was to be able to more carefully define the region of the cluster over which to average the model velocity dispersion. In our models the velocity dispersion decreases with radius from the cluster center and the total velocity dispersion is rather sensitive to the choice of integration region. For example, increasing the integration region from 7.'5 to 20′ reduced the calculated model velocity dispersion by 15% and consequently increased the mass estimate by some 30%.

The results are shown in Figure 3 as the band stretching along the $kT_{\rm AVE}$ axis. The numerical value derived from the galaxy dynamics is $\rho_0 = (1.19[+0.51; -0.27]) \times 10^{-25}$ g cm^{-3}. This value is consistent with the X-ray–determined one at the 68% confidence level. When the X-ray and optically determined values are combined we derive a value of $\rho_0 = (0.94[+0.27; -0.15]) \times 10^{-25}$ g cm^{-3} (68% confidence).

5. DISCUSSION AND CONCLUSIONS

We have presented a detailed analysis of the X-ray spectrum of the Abell 665 cluster of galaxies. We find consistency between the *Einstein Observatory* data and data obtained by the *Ginga* satellite. Joint fitting of these data sets allows us to set strong limits on the polytropic index ($\gamma < 1.35$ at 99% confidence), under the assumption that the temperature distribution is polytropic. The best fit is the isothermal case. We have also determined the average temperature, the hydrogen column density to the source, the iron abundance, the emission measure, and the relative normalization between the data sets. We have examined the effect of systematic errors due to gain and background subtraction.

A665 is very similar to the Coma Cluster in many of the properties of its gaseous atmosphere. The average temperatures of the two clusters are similar (7.5 keV for Coma vs. 8.3 keV for A665). The luminosities are comparable: 8.8×10^{44} ergs s^{-1} for Coma and 1.5×10^{45} ergs s^{-1} for A665. The core radii (305 kpc vs. 380 kpc) and β values (0.63 vs. 0.66) from the X-ray surface brightness distributions are also nearly the same. And in addition, when a detailed model for the distribution of mass in these clusters is constructed we find that A665 is very likely as massive as the Coma Cluster.

The values of the total cluster mass for A665 inferred from the X-ray spectrum and the galaxy dynamics are consistent at the 68% confidence level. Oegerle et al. (1991) discuss a slight inconsistency for A665 between $\beta_{\rm spec}$, the ratio of gas to galaxy scale heights, and $\beta_{\rm fit}$, the slope of the X-ray surface brightness distribution at large radii. For the velocity dispersion value we used to estimate the cluster mass, $\beta_{\rm spec} = 0.97(+0.50; -0.27)$.

This is only different at the 1.1 σ level from the $\beta_{\rm fit}$ value of 0.66 and so no strong conclusion is possible. Only when a considerably larger number of galaxy redshifts are available will it be possible to make an accurate comparison between $\beta_{\rm spec}$ and $\beta_{\rm fit}$.

Within a radius of 2 Mpc (about 8.5) the virial mass of A665 is $1.01(+0.29; -0.16) \times 10^{15}\ M_\odot$, the gas mass is $2.76(+0.07; -0.12) \times 10^{14}\ M_\odot$, and the visual luminosity of the galaxies is approximately $1.2 \times 10^{13}\ L_\odot$ (Dressler 1978). This implies a ratio of gas mass to virial mass of $0.27(+0.06; -0.07)$ and a mass-to-light ratio of $97(+28; -15)$ in solar units, values which are consistent with those found in other massive rich clusters of galaxies. When we convert our optical luminosity to stellar mass using a mass-to-light ratio of 5 (M/L_V; Pickles 1985), we find that the gas mass to stellar mass ratio is 4.6, again consistent with what one expects for a massive cluster.

The Hopkins Ultraviolet Telescope (HUT) observed A665 to search for ultraviolet photons from the decay of massive neutrinos, which have been suggested as a candidate for the dark matter in clusters of galaxies (Sciama 1991). No clear spectral line feature which could be associated with the purported decay photons was observed. We have integrated our virial mass profile over the HUT aperture (17″ × 116″) to obtain a total mass from A665 within this region of $2.23(+0.64; -0.36) \times 10^{13}\ M_\odot$. A significant fraction of this mass is baryonic: the X-ray emitting gas is $0.34 \times 10^{13}\ M_\odot$ and the mass in galaxies is $0.07 \times 10^{13}\ M_\odot$, leaving $1.82(+0.64; -0.36) \times 10^{13}\ M_\odot$ which could potentially be composed of massive neutrinos. Davidsen et al. (1991) conclude that Sciama's theory of decaying massive neutrinos could survive only if A665 were several times less massive than they estimated or if there were substantial UV absorption along the line of sight. Our analysis here indicates that the cluster's mass is about 60% of the value used by Davidsen et al. (1991). This, by itself, is not a sufficient enough reduction in the cluster's mass to bring the HUT observations into agreement with Sciama's theory.

We find a rather high elemental abundance 0.49 ± 0.16 (fraction relative to cosmic) for this cluster. Recent work with *Ginga* and *EXOSAT* (Hatsukade 1989; Arnaud et al. 1992) has found a correlation of iron abundance and gas temperature: hotter clusters show lower iron abundance than cooler ones. Their correlation would suggest an elemental abundance of 0.28 for a temperature of 8.3 keV, a value which is somewhat inconsistent (at about the 95% confidence level) with the A665 data presented here. The abundance-temperature correlation has been interpreted in the following manner: since there is known to be more gas per stellar mass in richer (or hotter) clusters (David et al. 1990), the iron (which is assumed to be produced by the cluster stellar population) is more diluted in the hotter clusters (David, Forman, & Jones 1991). However, Arnaud et al. (1992) showed that the iron mass in clusters is correlated with the stellar mass in elliptical and S0 galaxies; no correlation was observed for spirals. Research into the current galaxy population of A665 may help us to investigate further this apparent discrepancy.

The results from this spectral study have been used to determine the Hubble constant (and associated observational uncertainties) from the SZ effect (BHA). In that work we find the best-fit value to be $H_0 = (40\text{–}50) \pm 12$ km s^{-1} Mpc^{-1} where the range expresses the maximum range of systematic errors associated with the zero level uncertainty in the SZ data and the other systematic errors have been added in quadrature to the random error. However, the systematic errors dominate the statistical error and the worst case (most conservative) estimate gives a range of 26 ± 8 to 65 ± 10 km s^{-1} Mpc^{-1} for the Hubble constant. A significant component of that error arises from the measurement of X-ray temperature. The next Japanese X-ray astronomy satellite (*Astro-D*), scheduled for launch in early 1993, will be able to determine the X-ray spectra of distant ($z \sim 0.2$) clusters with high precision. Until then improvement in the uncertainty on the Hubble constant determination awaits reduction in the systematic errors associated with the radio measurements. Deep images with *ROSAT*, in addition to the structural information, will allow improved determination of the low energy (0.2–2 keV) X-ray spectrum of the cluster. As we have shown in this paper, this is an essential feature for characterizing the X-ray spectrum and constraining the temperature distributions in distant galaxy clusters.

J. P. H. acknowledges support from NASA grants NAG8-699 and NAG8-181.

REFERENCES

Abell, G. O. 1958, ApJS, 3, 211
Abramopoulos, F., & Ku, W. H.-M. 1983, ApJ, 271, 446
Arnaud, M., Rothenflug, R., Boulade, O., Vigroux, L., & Vangioni-Flam, E. 1992, A&A, 254, 49
Birkinshaw, M. 1979, MNRAS, 187, 847
———. 1989, in The Cosmic Microwave Background: 25 Years Later, ed. N. Mandolesi, & N. Vittorio (Dordrecht: Kluwer), 77
Birkinshaw, M., Hughes, J. P., & Arnaud, K. A. 1991, ApJ, 379, 466 (BHA)
Boynton, P. E., Radford, S. J. E., Schommer, R. A., & Murray, S. S. 1982, ApJ, 257, 473
Briel, U. G., Henry, J. P., & Böhringer, H. 1991, in Proc. NATO ASI on Clusters and Superclusters of Galaxies (Contributed Talks and Poster Papers), ed. M. M. Colless et al., 91
David, L. P., Arnaud, K. A., Forman, W., & Jones, C. 1990, ApJ, 356, 32
David, L. P., Forman, W., & Jones, C. 1991, ApJ, 380, 39
Davidsen, A. F., et al. 1991, Nature, 351, 128
Dressler, A. 1978, ApJ, 226, 55
Edge, A. C. 1989, Ph.D. thesis, University of Leicester
Edge, A. C., & Stewart, G. C. MNRAS, 252, 428
Geller, M. J., & Beers, T. C. 1982, ApJ, 94, 421
Gioia, I. M., Maccacaro, T., Schild, R. E., Wolter, A., Stocke, J. T., Morris, S. L., & Henry, J. P. 1990, ApJS, 72, 567
Harris, D. E., et al. 1990, The *Einstein Observatory* Catalog of IPC X-Ray Sources (NASA RP-1247)
Hatsukade, I. 1989, Ph.D. thesis, Osaka University
Hayashida, K., et al. 1989, PASJ, 41, 373
Henriksen, M. J., & Mushotzky, R. F. 1986, ApJ, 302, 287
Hughes, J. P. 1989, ApJ, 337, 21
Jones, C., & Forman, W. 1984, ApJ, 276, 38
King, I. R. 1966, AJ, 71, 64
Makino, F., & the Astro-C team 1987, Astrophys. Lett. & Comm., 25, 223
Merritt, D. 1987, ApJ, 313, 121
Mushotzky, R. F. 1988, in Proc. NATO ASI: Hot Thin Plasmas in Astrophysics, ed. R. Pallavacini (Dordrecht: Reidel), 273
Oegerle, W. R., Fitchett, M. J., Hill, J. M., & Hintzen, P. 1991, ApJ, 376, 46
Pickles, A. J. 1985, ApJ, 296, 340
Raymond, J. C., & Smith, B. W. 1977, ApJS, 35, 419 (RS)
Sciama, D. W. 1991, ApJ, 367, L39
Stark, A. A., Heiles, C., Bally, J., & Linke, R. 1984, privately distributed magnetic tape
The, L. S., & White, S. D. M. 1986, AJ, 92, 1248
Turner, M. J. L., et al. 1989, PASJ, 41, 345
White, S. D. M., & Silk, J. 1980, ApJ, 241, 864